

Optimal Method for Polarization Selection of Stationary Objects Against the Background of the Earth's Surface

Valerii Volosyuk, Simeon Zhyla, Vladimir Pavlikov, Nikolay Ruzhentsev, Eduard Tserne, Anatoliy Popov, Oleksandr Shmatko, Kostiantyn Dergachov, Olena Havrylenko, Ivan Ostroumov, Nataliia Kuzmenko, Olga Sushchenko, Yuliya Averyanova, Maksym Zaliskyi, Oleksandr Solomentsev, Borys Kuznetsov, and Tatyana Nikitina

Abstract—Within the maximum likelihood method an optimal algorithm for polarization target selection against the background of interfering signal reflected from the earth's surface is synthesized. The algorithm contains joint operations of spectral interference rejection and their polarization compensation by means of certain combinations of interchannel subtraction of signals of different polarizations. The physical features of the elements of the polarization scattering matrix are investigated for the technical implementation of the synthesized algorithm.

Keywords—polarimetric radar; polarization selection; power lines detection; multichannel processing; maximum likelihood method

I. INTRODUCTION

FOR many decades the problem of selection various, especially small-sized, objects against the background of the earth's surface remains relevant in radar [1]–[5]. The

This work was supported by the Ministry of Education and Science of Ukraine; the state registration numbers are 0120U10208 and 0119U100968.

V. Volosyuk, S. Zhyla, V. Pavlikov, N. Ruzhentsev, E. Tserne are with Department of aerospace radio-electronic systems National Aerospace University H.E. Zhukovsky "Kharkiv Aviation Institute", Ukraine (e-mail: v.volosyuk@khai.edu, s.zhyla@khai.edu, v.pavlikov@khai.edu, e.tserne@khai.edu).

A. Popov is with Department of Radio-Electronic and Biomedical Computerized Means and Technologies National Aerospace University H.E. Zhukovsky "Kharkiv Aviation Institute", Ukraine (e-mail: a.v.popov@khai.edu).

O. Shmatko is with Laboratory of electron microscopy, optics, and laser technologies National Aerospace University H.E. Zhukovsky "Kharkiv Aviation Institute", Ukraine (e-mail: o.shmatko@khai.edu).

K. Dergachov, O. Havrylenko are with Aircraft Control Systems Department National Aerospace University H.E. Zhukovsky "Kharkiv Aviation Institute", Ukraine (e-mail: k.dergachov@khai.edu, o.havrylenko@khai.edu).

I. Ostroumov, N. Kuzmenko, O. Sushchenko, Y. Averyanova are with Air Navigation Systems Department National Aviation University, Ukraine (e-mail: ayua@nau.edu.ua).

M. Zaliskyi, O. Solomentsev are with Department of telecommunication and radioelectronic systems National Aviation University, Ukraine (e-mail: maximus2812, avsolomentsev@ukr.net).

B. Kuznetsov is with Magnetic Field Control Problems Department, State Institution "Institute of Technical Problems of Magnetism of the National Academy of Sciences of Ukraine", Ukraine (e-mail: kuznetsov.boris.i@gmail.com).

T. Nikitina is with Technical Disciplines Department, Kharkiv National Automobile and Highway University, Ukraine (e-mail: tat-jana55555@gmail.com).

existing means of Doppler selection of moving targets that have a relatively high efficiency in detecting low-flying targets in ground-based radars are not always applicable in airborne radars due to the complex nature and relatively large width of the Doppler frequency spectrum of interfering reflections from the earth's surface. Therefore it is of practical interest to study the possibilities of using not only Doppler but also other distinctive features of signals reflected from the earth's surface and selectable moving and stationary targets, in particular, from power lines that pose a serious threat to helicopter flights at low altitudes. These can be polarization distinctive features, differences in the delay times of reflected useful signals and interference, differences angular coordinates, intensity, texture differences, etc [6]–[10].

In this paper, a case of the use of polarization distinctive features is considered and the problem of developing new optimal method for selection stationary targets against the background of the earth's surface is solved within the the maximum likelihood method [11]–[14]. When selecting stationary targets, for example power lines, the use of Doppler distinctive features is not possible because the spectra of signals reflected from the earth's surface and the spectrum of the useful signal overlap significantly. In these cases additional use of polarization differences is of interest. To perform the selection of signals reflected from power lines it is advisable to use the fact that the power lines will reflect polarized signals [15]–[17] with directions of polarization coinciding mainly with the directions of the wires.

II. PROBLEM STATEMENT, INITIAL DATA AND THEIR STATISTICAL ANALYSIS

To solve the optimization problem the transmitted signal will be represented in the following mathematical form

$$s_{\mu}(t) = \text{Re} \dot{S}_{0\mu}(t) \exp(j2\pi f_0 t), \quad (1)$$

where $\dot{S}_{0\mu}(t)$ is the complex envelope of the transmitted signal, $\mu = (V, H)$ is the polarization index, f_0 is the carrier frequency. This form of signal presentation characterizes a large class of narrowband and wideband signals. We will



assume that the complex envelopes of the transmitted signals are the same at both polarizations, i.e. $\dot{S}_{0\mu}(t) = \dot{S}_0(t)$.

The received signal can be represented as the additive model

$$\vec{u}(t) = \|u_k(t)\| = \vec{s}(t, \vec{\lambda}) + \vec{n}(t) + \vec{\eta}(t), \quad t \in (0, T), \quad (2)$$

where the useful signal $\vec{s}(t, \vec{\lambda}) = \|s_k(t, \vec{\lambda})\|$ has a functionally deterministic form [18]–[20] with respect to time t and parameters $\vec{\lambda} = \|\lambda_\nu\|$, interference includes signals $\vec{n}(t) = \|n_k(t, \vec{\lambda})\|$ reflected from the earth's surface and internal white Gaussian noise $\vec{\eta}(t) = \|\eta_k(t)\|$. The index $k = \overline{1, 2} = (VV, HH)$, as well as the indices i and j below correspond to the type of polarization of the received oscillations (first letter) at a given polarization of the transmitted ones (second letter).

The structure of the useful signal reflected from the selectable object has the following form

$$s_k(t, \vec{\lambda}) = \text{Re} \dot{S}_{0k} [t - t_{del}(t), \vec{\lambda}] e^{j\omega_0[t - t_{del}(t)]}. \quad (3)$$

In the simplest case, a set of parameters $\vec{\lambda} = [t_{del}(R_{obj}, \nu, t), \omega_{obj}(\nu), \phi_{obj}]$ characterizes the position of the target. These are the range R_{obj} and speed ν associated with delay time t_{del} and Doppler frequency shift ω_{obj} , as well as angular coordinates ϕ_{obj} . Obviously, for effective polarization selection of useful signals against the background of interference, they must have clearly pronounced corresponding differences. Obviously pronounced polarization differences have interference reflections from the earth's surface and, for example signals reflected from the wires of power lines, as the polarization of these signals will match their direction. High-speed targets will have pronounced Doppler differences.

The interference signal formed by the reflections of waves from many elements of the earth's surface can be written in the following form [21], [22]

$$n_k(t) = \text{Re} \dot{C} \int_D \dot{G}(\vec{r}, t) \dot{F}_k(\vec{r}, t) \dot{S}_0 [t - t_{del}(t, \vec{r})] \times e^{j\omega_0[t - t_{del}(t, \vec{r})]} d\vec{r}, \quad (4)$$

where \dot{C} is the proportionality coefficient, including attenuation of signals along the path of their propagation, transmission coefficients of antenna-feeder paths, etc.; $\dot{G}(\vec{r}, t)$ is the directional diagram of the antenna, which illuminates the surface with its beam; $\dot{F}_k(\vec{r}, t)$ is the complex coefficient (specific) of reflection (scattering) of waves from elementary surface areas.

Within the correlation theory the statistical characteristics of interfering reflections of various polarizations are represented by the matrix

$$\underline{R}_n(t_1, t_2) = \|R_{n\ ij}(t_1, t_2)\| = \begin{vmatrix} \langle n_{VV}(t_1)n_{VV}(t_2) \rangle & \langle n_{VV}(t_1)n_{HH}(t_2) \rangle \\ \langle n_{HH}(t_1)n_{VV}(t_2) \rangle & \langle n_{HH}(t_1)n_{HH}(t_2) \rangle \end{vmatrix}. \quad (5)$$

The elements of this matrix are correlation and cross-correlation functions of the following form:

$$R_{n\ ij}(t_1 - t_2) \approx \sigma_{ij}^o r_{Fij}(t_1 - t_2) r_G(t_1 - t_2) \psi_0(t_1 - t_2), \quad (6)$$

where $r_{Fij}(t_1 - t_2)$ is the normalized correlation function of the signals reflected from chaotically moving surface elements;

$r_G(t_1 - t_2)$ is the normalized correlation function practically independent on the type of polarization and caused by multiple Doppler frequency shifts during signal reflections from surface elements located at different angles with respect to the velocity vector of the aircraft in the range of angles of the directional diagram; σ_{ij}^o is the radar cross section [23],

$$\psi_0(t_1 - t_2) = 0,5 \text{Re} \left\{ e^{j\omega_0(t_1 - t_2)} \dot{\Psi}_0(t_1 - t_2) \right\}, \quad (7)$$

$$\dot{\Psi}_0(t_1 - t_2) = \int_{-\infty}^{\infty} \dot{S}_0 [t_1 - t_{del}] \dot{S}_0^* [t_2 - t_{del}] dt_{del}. \quad (8)$$

III. OPTIMAL METHOD SYNTHESIS

Within the statistical theory of processing Gaussian random processes for a functionally deterministic model of the useful received signal [24], the solution of the optimization problem of polarization target selection is found by the maximum likelihood method, differentiating and equating to zero the likelihood functional

$$\frac{\partial}{\partial \lambda_i} P [\vec{u} | \vec{s}(t, \vec{\lambda})] = 0, \quad (9)$$

where

$$P [\vec{u} | \vec{s}(t, \vec{\lambda})] = \kappa \exp \left\{ -\frac{1}{2} \int_0^T \int_0^T [\vec{u}^T(t_1) - \vec{s}^T(t_1, \vec{\lambda})] \underline{W}(t_1, t_2) [\vec{u}(t_2) - \vec{s}(t_2, \vec{\lambda})] dt_1 dt_2 \right\}, \quad (10)$$

$\underline{W}(t_1, t_2) = \|W_{ij}(t_1, t_2)\|$ is the inverse matrix of inverse correlation functions that can be found from the integral and matrix inversion equation

$$\int_0^T \underline{R}_{\Sigma}(t_1, t_2) \underline{W}(t_2, t_3) dt_2 = \underline{I} \delta(t_1 - t_3), \quad (11)$$

$\delta(t_1 - t_3)$ is the delta function, \underline{I} is the unit matrix,

$$\underline{R}_{\Sigma}(t_1, t_2) = \underline{R}_n(t_1 - t_2) + \underline{R}_{\eta}(t_1 - t_2) = \|\sigma_{ij}^o r_{Fij}(t_1 - t_2) r_G(t_1 - t_2) \psi_0(t_1 - t_2)\| + 0,5 \underline{N}_{0\eta} \delta(t_1 - t_2) \quad (12)$$

is the total correlation function of the earth's interference and internal noise of receivers, $N_{0\eta 1}$ and $N_{0\eta 2}$ are power spectral densities of the internal noises in every receiver channels.

Likelihood functional (10) is transformed to the following form

$$P [\vec{u} | \vec{s}(t, \vec{\lambda})] = \kappa \kappa_1 e^{Y(\vec{\lambda})} e^{-\mu(\vec{\lambda})}, \quad (13)$$

$$\kappa_1 = \exp \left\{ -\frac{1}{2} \int_0^T \int_0^T \vec{u}^T(t_1) \underline{W}(t_1, t_2) \vec{u}(t_2) dt_1 dt_2 \right\}, \quad (14)$$

$$Y(\vec{\lambda}) = \int_0^T \int_0^T \vec{u}^T(t_1) \underline{W}(t_1, t_2) \vec{s}(t_2, \vec{\lambda}) dt_1 dt_2, \quad (15)$$

$$\mu[\vec{s}(t, \vec{\lambda})] = \frac{1}{2} \int_0^T \int_0^T \vec{s}^T(t_2, \vec{\lambda}) \underline{W}(t_1, t_2) \vec{s}(t_2, \vec{\lambda}) dt_1 dt_2. \quad (16)$$

The functional $\mu[\vec{s}(t, \vec{\lambda})]$, which depends on the ratio of the signal and noise energies, does not depend on the parameters $\vec{\lambda}$, since its main parameters are not energetic. Then the factor $e^{-\mu(\vec{\lambda})} = k_2 = const$ and instead of searching for the maximum of functional (10) on a set of unknown parameters $\vec{\lambda}$ it is necessary to find the maximum of the factor $e^{Y(\vec{\lambda})}$ or the output effect $Y(\vec{\lambda})$ monotonically related to it.

In the coordinate form, the output effect (15) indicates all the necessary algorithmic operations for received signals processing

$$Y(t_{del}, \vec{\lambda}) = \sum_{i=1}^2 \sum_{j=1}^2 \int_0^T \int_0^T u_i(t_1) W_{ij}(t_1, t_2) \times s_j(t_2 - t_{del}, \vec{\lambda}) dt_1 dt_2. \quad (17)$$

With a specific physical content of (17) the circuit-technical and software-algorithmic implementation of this expression and the determination of its maximum on a set of parameters $\vec{\lambda}$ is sufficient to solve the posed problem of polarization objects selection. Expression (17) presented in general form as an algorithm contains the actions of both polarization and spectral selection of moving objects in the presence of corresponding polarization differences and differences in the Doppler shifts of the frequencies of useful signals and interference.

For further research, it is advisable to represent this expression in the spectral form

$$\begin{aligned} \dot{Y}(j\omega, \vec{\lambda}) &= \sum_{i=1}^2 \sum_{j=1}^2 \dot{U}_i(j\omega) \dot{G}_{W_{ij}}^*(\omega) \dot{S}_j^*(j\omega) = \\ &= \dot{U}_{VV}(j\omega) \dot{G}_{W_{11}}(\omega) \dot{S}_{VV}^*(j\omega) + \\ &+ \dot{U}_{VV}(j\omega) \dot{G}_{W_{12}}^*(\omega) \dot{S}_{HH}^*(j\omega) + \\ &+ \dot{U}_{HH}(j\omega) \dot{G}_{W_{21}}^*(\omega) \dot{S}_{VV}^*(j\omega) + \\ &+ \dot{U}_{HH}(j\omega) \dot{G}_{W_{22}}(\omega) \dot{S}_{HH}^*(j\omega), \end{aligned} \quad (18)$$

where $\dot{G}_{W_{ij}}^*(\omega)$ is the element of inverse matrix of interference energy spectrum $\dot{G}_W(\omega) = \dot{G}_{R\Sigma}^{-1}(\omega)$, $\dot{G}_{R\Sigma}(\omega) = F\{R_\Sigma(t_1 - t_2)\}$, $F\{\cdot\}$ is the Fourier operator,

$$\dot{G}_W(\omega) = \Delta^{-1} \times \begin{vmatrix} \sigma_{22}^o G_{n22}(\omega) + \frac{1}{2} N_{0\eta 2} & -\sigma_{12}^o \dot{G}_{n12}(\omega) \\ -\sigma_{21}^o \dot{G}_{n21}(\omega) & \sigma_{11}^o G_{n11}(\omega) + \frac{1}{2} N_{0\eta 1} \end{vmatrix}, \quad (19)$$

$$\Delta = \sigma_{11}^o \sigma_{22}^o G_{n11} G_{n22} + \sigma_{11}^o G_{n11} \frac{N_{0\eta 2}}{2} + \sigma_{22}^o G_{n22} \frac{N_{0\eta 1}}{2} + \frac{N_{0\eta 1} N_{0\eta 2}}{4} - \sigma_{12}^o \sigma_{21}^o \dot{G}_{n12} \dot{G}_{n21} \quad (20)$$

is the determinant of the matrix $\dot{G}_{R\Sigma}(\omega)$, $\dot{U}_i(j\omega)$ is the spectrum of $u_i(t)$, $\dot{S}_j^*(j\omega)$ is the spectrum of $s_j(t_2 - t_{del}, \vec{\lambda})$.

In a concretized form equation (18) takes the following form

$$\begin{aligned} \dot{Y}(j\omega, \vec{\lambda}) &= \{\dot{U}_{VV}(j\omega)(\sigma_{22}^o G_{n22}(\omega) + 0,5N_{0\eta 2})\Delta^{-1} - \\ &- \dot{U}_{HH}(j\omega) \sigma_{21}^o \dot{G}_{n21}^*(\omega) \Delta^{-1}\} \dot{S}_{VV}^*(j\omega) + \\ &+ \{\dot{U}_{HH}(j\omega)(\sigma_{11}^o G_{n11}(\omega) + 0,5N_{0\eta 1})\Delta^{-1} - \\ &- \dot{U}_{VV}(j\omega) \sigma_{12}^o \dot{G}_{n12}^*(\omega) \Delta^{-1}\} \dot{S}_{HH}^*(j\omega). \end{aligned} \quad (21)$$

In the Fig. 1 it is shown a scheme that implements the optimal output effect of polarization-Doppler target selection represented by expression (21). This block diagram should

include a measuring unit for the elements of the scattering covariance matrix

$$\|\dot{\sigma}_{ij}^o\| = \left\| \begin{vmatrix} \dot{\sigma}_{11}^o & \dot{\sigma}_{12}^o \\ \dot{\sigma}_{21}^o & \dot{\sigma}_{22}^o \end{vmatrix} \right\|. \quad (22)$$

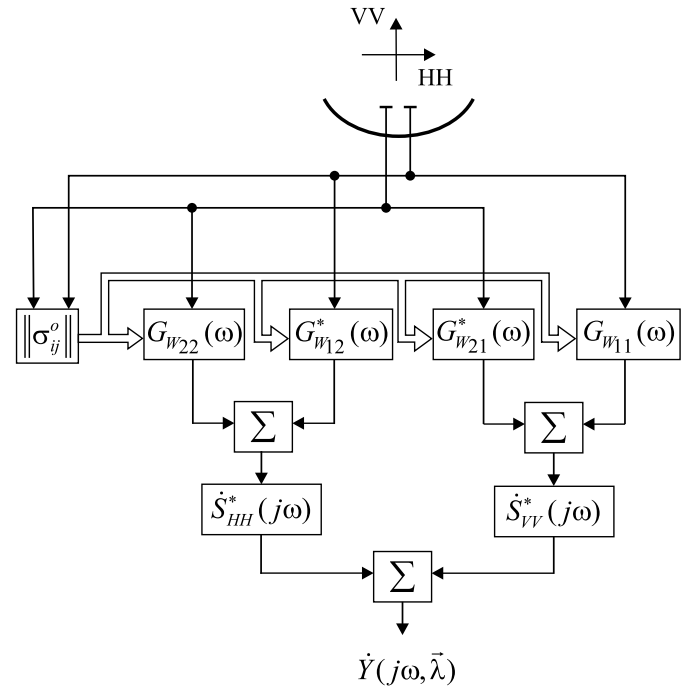


Fig. 1. Block diagram of the polarization-Doppler target selection system

Matched filtering of signals reflected from selectable targets occurs in blocks $\dot{S}_{VV}^*(j\omega)$ and $\dot{S}_{HH}^*(j\omega)$, Doppler spectral rejection of interference in blocks $\dot{G}_{W_{ij}}^*(\omega)$ and polarization compensation in adders, which take signals of different polarizations of opposite signs with appropriate weight coefficients equalizing their root-mean square values. Thus, the obtained algorithm and the corresponding scheme contain operations and devices for mixed polarization and spectral Doppler interference compensation and the extraction of useful signals from the background radiation.

IV. ANALYSIS OF THE DEVELOPED METHOD

To clarify physical essence of the method (21) and operation principles of polarization selection it is advisable to additionally introduce some simplifications and assumptions that do not significantly affect the efficiency of the problem solution and its physical and algorithmic essence, but significantly simplify the mathematical calculations.

From the analysis of the obtained method (21) it follows that the main operations of the received signals processing depend on the form of the correlation function (6) and its spectral representation. It is necessary to analyze the physical features of the correlation of interference signals at different polarizations.

It can be assumed that if the reflected oscillations of different polarizations are weakly correlated then in this case the normalized correlation functions with different indices

may also differ significantly. Such a case can occur when the reflected signals are formed by various surface elements, for example, thin stems of vegetation with a predominantly vertical or horizontal position and reacting differently to random gusts of wind. If fluctuations in vertical and horizontal polarizations are created by the same surface elements, (for example, leaves with comparable dimensions in length and width, or the same thin stems of vegetation, but with certain slopes not with strict horizontal or vertical orientations), then a high correlation of reflected signals of different polarizations and real practically identical (independent of index numbers) functions should be expected. Note that it is the case of high correlation of oscillations of different polarizations that is of practical interest, since only when they are highly correlated there is effective compensation for interference reflections from the earth's surface. With zero correlation there is no interference compensation.

Note also that in (6) the autocorrelation functions $r_{Fii}(t_1 - t_2)$ and $r_{Fjj}(t_1 - t_2)$ are even with maxima at the values of the arguments $(t_1 - t_2)$. In the general case, the form of mutual correlation functions $r_{Fij}(t_1 - t_2)$ can differ significantly from the form of autocorrelation functions. They can be asymmetric and their maxima can be at the values of the variables $t_1 \neq t_2$. However, from simple physical considerations, it can be assumed that since the reflected oscillations of different polarizations are formed to a large extent by practically the same surface elements, the maxima of the mutual correlation functions are at the same points as the maxima of the autocorrelation functions. In addition, it can be assumed that with a high degree of correlation of oscillations of different polarizations, the forms of the mutual correlation functions are close to the forms of autocorrelation and are even. In this case, the effective mutual scattering cross sections σ_{ij}^o can be considered real, and the function

$$r_{Fij}(t_1 - t_2) \approx r_F(t_1 - t_2) \quad (23)$$

is real and independent on the type of polarization of the received signals.

The total correlation function can be represented as follows

$$\begin{aligned} R_{\Sigma ij}(t_1 - t_2) &= \\ &= \sigma_{ij}^o \varphi(t_1 - t_2) + 0,5N_{0\eta_i} \delta(t_1 - t_2) = \\ &= \sqrt{\sigma_i^o \sigma_j^o} r_{ij} \varphi(t_1 - t_2) + 0,5N_{0\eta_i} \delta(t_1 - t_2), \end{aligned} \quad (24)$$

where $\varphi(t_1 - t_2) = r_F(t_1 - t_2) r_G(t_1 - t_2) \psi_0(t_1 - t_2)$, $\sigma_{ij}^o = \sqrt{\sigma_i^o \sigma_j^o} r_{ij}$, r_{ij} is normalized correlation coefficient of received signals of different polarizations.

To clarify the physical essence of the obtained algorithm (21) we will assume that the channels for receiving the vertical and horizontal polarizations are identical with the same internal noise $N_{0\eta_1} = N_{0\eta_2} = N_0$. We also consider the structures of useful selectable signals to be the same $\dot{S}_{VV}(j\omega) = \dot{S}_{HH}(j\omega) = \dot{S}_0(j\omega)$. In this case, the output

effect of the optimal processing system is as follows

$$\begin{aligned} \dot{Y}(j\omega, \vec{\lambda}) &= U_{VV}(j\omega) \dot{S}_0^*(j\omega) \Delta^{-1} \times \\ &\times \{ \sigma_2^o G_\varphi(\omega) - \sqrt{\sigma_1^o \sigma_2^o} r_{12} G_\varphi(\omega) + 0,5N_{0\eta} \} - \\ &\quad - \dot{U}_{HH}(j\omega) \dot{S}_0^*(j\omega) \Delta^{-1} \times \\ &\times \{ \sqrt{\sigma_2^o \sigma_1^o} r_{21} G_\varphi(\omega) - \sigma_1^o G_\varphi(\omega) + 0,5N_{0\eta} \}. \end{aligned} \quad (25)$$

It is necessary to analyze the synthesized algorithm in two limiting cases. In the first case it is assumed that the internal noise $\eta_i(t) = 0$ and correlation coefficients $r_{12} = r_{21} = 1$. The equality $r_{12} = r_{21} = 1$ is valid, for example, for the models of small-scale and large-scale surfaces and indicates the synchronism in time of fluctuations of signals of different polarizations reflected from the same chaotically moving elements of a randomly inhomogeneous surface. Then there is a complete compensation of the interference, which indicates the operability of the algorithm, in which the main operation is the weight subtraction of signals of different polarizations

$$\begin{aligned} \dot{Y}_1(j\omega, \vec{\lambda}) &= \\ &= U_{VV}(j\omega) \dot{S}_0^*(j\omega) G_\varphi(\omega) \Delta^{-1} \{ \sigma_2^o - \sqrt{\sigma_1^o \sigma_2^o} \} + \\ &\quad + \dot{U}_{HH}(j\omega) \dot{S}_0^*(j\omega) G_\varphi(\omega) \Delta^{-1} \{ \sigma_1^o - \sqrt{\sigma_1^o \sigma_2^o} \}. \end{aligned} \quad (26)$$

In the second limiting case, we assume that only the first condition is satisfied, $\eta_i(t) = 0$. Then

$$\begin{aligned} \dot{Y}_1(j\omega, \vec{\lambda}) &= U_{VV}(j\omega) \dot{S}_0^*(j\omega) G_\varphi(\omega) \Delta^{-1} \times \\ &\quad \times \{ \sigma_2^o - \sqrt{\sigma_1^o \sigma_2^o} r_{12} \} + \\ &\quad + \dot{U}_{HH}(j\omega) \dot{S}_0^*(j\omega) G_\varphi(\omega) \Delta^{-1} \{ \sigma_1^o - \sqrt{\sigma_1^o \sigma_2^o} r_{21} \}. \end{aligned} \quad (27)$$

The factor $\dot{S}_0^*(j\omega) G_\varphi(\omega) \Delta^{-1}$ in (25) and (26) corresponds to Doppler selection that contains operations of matched filtering (multiplication by $\dot{S}_0^*(j\omega)$) and operations of spectral rejection of interference by decorrelation $G_\varphi(\omega) \Delta^{-1}$ or, which is the same, by creating a dip in the amplitude-frequency characteristic of the receiver in the frequency range occupied by the interference G_φ . The expression in curly braces and partially the structure of the determinant Δ is mainly responsible for polarization selection.

V. ANALYSIS OF THE ACCURACY OF POLARIZATION SELECTION

To analyze the degree of polarization compensation of the background radiation of the earth the equation (27) is written in the form of residual interference from the earth

$$\begin{aligned} \Delta n_{resid}(t) &= (\sigma_2^o - \sqrt{\sigma_1^o \sigma_2^o} r_{12}) n_{VV}(t) + \\ &\quad + (\sigma_1^o - \sqrt{\sigma_1^o \sigma_2^o} r_{21}) n_{HH}(t), \end{aligned} \quad (28)$$

where $n_i(t) = \sigma_i^o \nu_i(t)$, $\nu_i(t)$ are mutually uncorrelated random processes with unit variance.

The dispersion of the residual noise after compensation has the following form

$$\sigma_{resid}^2 = \sigma_1^o \{ (1 - r^2) [1 + \alpha^2 - 2\alpha r] \}, \quad (29)$$

where $\alpha = \sqrt{\frac{\sigma_1^o}{\sigma_2^o}}$ is the ratio of the effective scattering cross-sections of reflected signals from the surface at different polarizations, $r_{12} = r_{21} = r$.

As a compensation coefficient for interference caused by reflections from the earth's surface, we take the function inverse to expression (29) and normalized to σ_1^o

$$\gamma(r, \alpha) = \frac{1}{(1 - r^2)[1 - 2\alpha r + \alpha^2]}. \quad (30)$$

The graphs of this function depending on the correlation coefficient r for various ratios α of the effective scattering cross-sections of the interference of various polarizations are shown in Fig. 2.

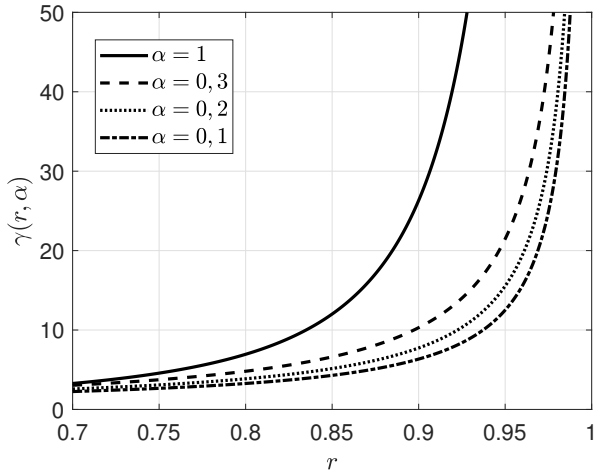


Fig. 2. Graphs of the compensation coefficient of interference reflections from the earth's surface $\gamma(r, \alpha)$

From the Fig. 2 it follows that the degree of interference compensation increases with an increase in the correlation coefficient r and it is maximum at $\alpha = 1$, i.e. with the same dispersion of interference reflections of different polarizations.

VI. SIMULATION MODELING OF THE POLARIZATION SELECTION ALGORITHM

Modeling of the operation of a radar with polarimetric selection of power lines was carried out in the Matlab software package. The model assumes that an antenna is located on board the aircraft, which is oriented in the direction of flight and performs an azimuth scan. Due to the small size of the onboard antenna and the wide beam of the directional pattern, not only power lines, but also the surface in the form of urban buildings, roads and steppe, fall into the observation area. The following flight parameters were chosen for the simulation: flight altitude $h = 500 \text{ m}$, range of elevation angles of the antenna directional pattern $\theta = 50^\circ \div 80^\circ$, pulse duration $\tau = 5 \text{ ns}$, resonant frequency of radiation $f_0 = 37 \text{ GHz}$, size of the onboard antenna $L = 20 \text{ cm}$. For the selected parameters, the calculation of the observation area, range resolution and elevation resolution were performed.

The model of the true radar image of the surface, which is usually adapted for the user by equalizing the contrasts, is shown in Fig. 3. Power lines are specially highlighted in yellow in the image.

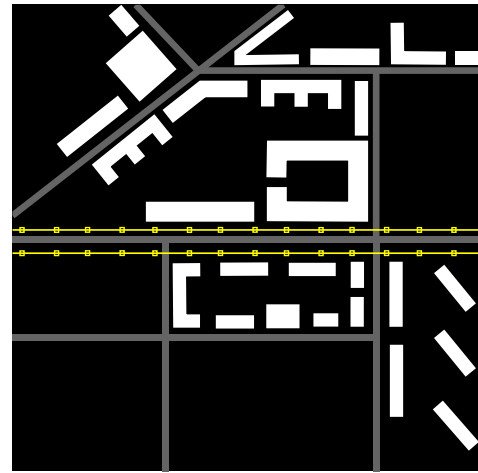


Fig. 3. Model of a true radar image with power lines (highlighted in yellow)

The model of the spatial distribution of radar cross section (RCS) over the surface at horizontal polarization for its various parts is shown in Fig. 4. Four types of surfaces were proposed and described on the Table I.

TABLE I
SURFACES PARAMETERS.

surface type	RCS model
steppe	$\sigma_1^o = \sigma_2^o = -\theta - 15 \text{ dB}$
concrete road	$\sigma_1^o = \sigma_2^o = -0.08 \cdot \theta - 29 \text{ dB}$
urban buildings	$\sigma_1^o = \sigma_2^o = -0.12 \cdot \theta - 14 \text{ dB}$
power lines	$\sigma_1^o = -0.3 \cdot \theta - 15 \text{ dB}$ $\sigma_2^o = -0.3 \cdot \theta - 10 \text{ dB}$

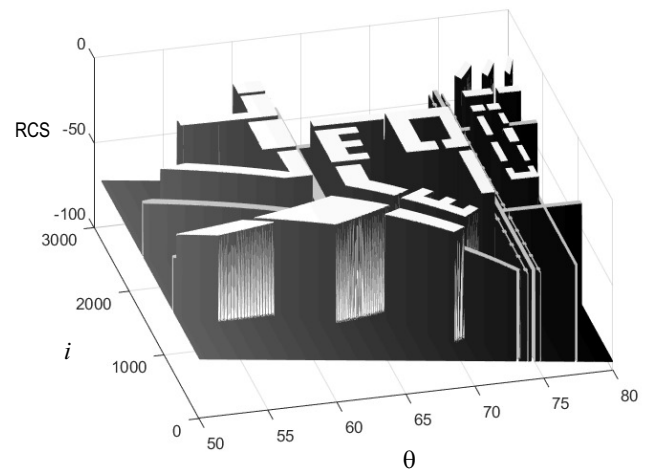


Fig. 4. Model of spatial distribution of RCS over the surface

In the Fig. 5 it is shown the residual noise on vertical polarization as a result of the primary processing of the received signals.

The result of applying the algorithm (27) with the correlation coefficient $r = 1$ is shown in Fig. 6. The obtained result

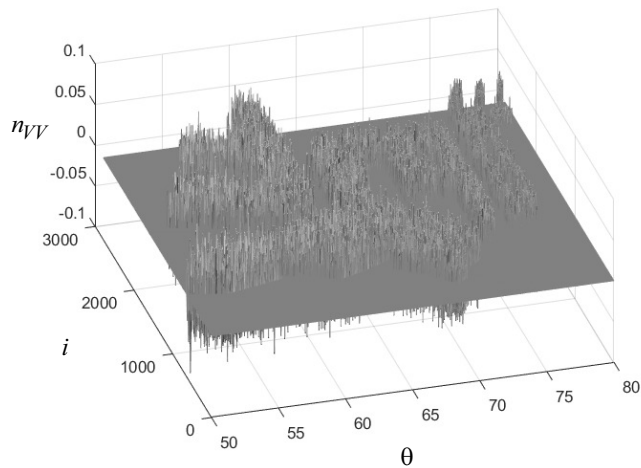


Fig. 5. Residual noise on vertical polarization as a result of primary processing

confirms the high degree of compensation, as shown in Fig. 2. If the correlation coefficient $r = 0,9$ then you can see in Fig. 7 uncompensated noise that will increase with decreasing r . Thus, the obtained theoretical results in Fig. 2 are fully confirmed by simulation modeling.

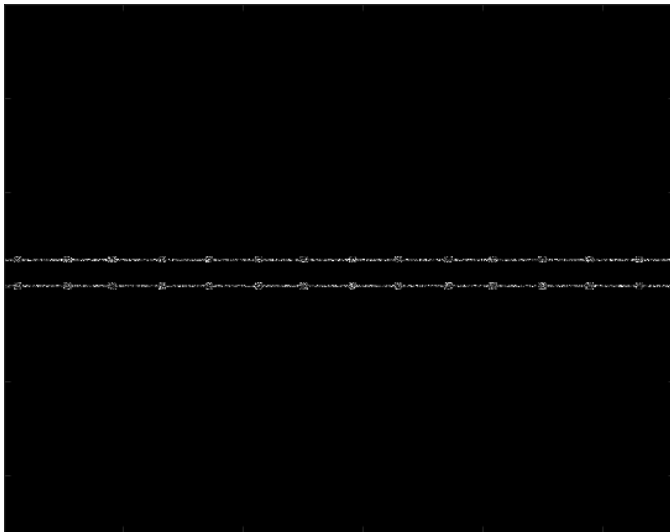


Fig. 6. Radar image of power lines for $r = 1$

VII. CONCLUSION

The algorithm of polarization target selection, synthesized within the maximum likelihood method, against the background of interfering reflections from the earth's surface, makes it possible to select targets based on the use of polarization distinctive features of reflected signals and sources of interference. The polarization selection algorithm, which contains certain combinations of interchannel signal subtraction, is distinguished by a significant novelty. A feature of the obtained algorithm is also the need to know the preliminary estimates of the elements of the polarization covariance matrix

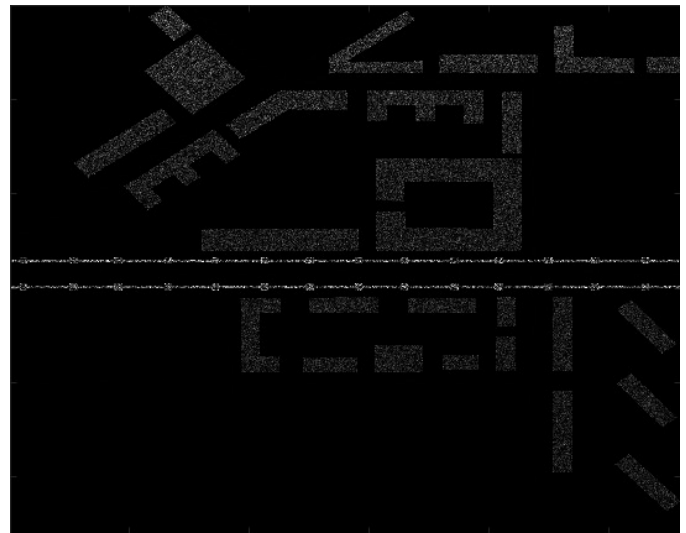


Fig. 7. Radar image of power lines for $r = 0,9$

of interference. In this regard, their physical characteristics were investigated with a high degree of correlation between interfering reflections of various polarizations. All the obtained results are confirmed by simulation modeling.

REFERENCES

- [1] H. Oriot and M. Flecheux, "Moving target detection using 2 SAR images," 2017 IEEE Radar Conference (RadarConf), Seattle, WA, USA, 2017, pp. 1064-1068, <https://doi.org/10.1109/RADAR.2017.7944362>.
- [2] H. Xu, Z. Yang, R. Zhang and G. Liao, "Shadow-aided method for ground slow moving targets detection of airborne high-resolution SAR images," 2015 IEEE 5th Asia-Pacific Conference on Synthetic Aperture Radar (APSAR), Singapore, 2015, pp. 831-834, <https://doi.org/10.1109/APSAR.2015.7306332>.
- [3] T. Leonard, T. Lamont-Smith, R. Hodges and P. Beasley, "94-GHz Tarsier radar measurements of wind waves and small targets," 2011 8th European Radar Conference, Manchester, UK, 2011, pp. 73-76.
- [4] Y. Zhang et al., "Demonstration of ocean target detection by Tiangong-2 interferometric imaging radar altimeter," 2018 22nd International Microwave and Radar Conference (MIKON), Poznan, Poland, 2018, pp. 261-264, <https://doi.org/10.23919/MIKON.2018.8405194>.
- [5] Chao-Hsiang Liao, Li-Der Fang, Powen Hsu and Dau-Chyrh Chang, "A UWB microwave imaging radar system for a small target detection," 2008 IEEE Antennas and Propagation Society International Symposium, San Diego, CA, USA, 2008, pp. 1-4, <https://doi.org/10.1109/APS.2008.4619667>.
- [6] J. Moulton, S. Kassam, F. Ahmad, M. Amin and K. Yemelyanov, "Target and change detection in synthetic aperture radar sensing of urban structures," 2008 IEEE Radar Conference, Rome, Italy, 2008, pp. 1-6, <https://doi.org/10.1109/RADAR.2008.4721104>.
- [7] C. Debes, A. M. Zoubir and M. G. Amin, "Enhanced Detection Using Target Polarization Signatures in Through-the-Wall Radar Imaging," in IEEE Transactions on Geoscience and Remote Sensing, vol. 50, no. 5, pp. 1968-1979, May 2012, <https://doi.org/10.1109/TGRS.2011.2170077>.
- [8] X. Mou, X. Chen, J. Guan, B. Chen and Y. Dong, "Marine Target Detection Based on Improved Faster R-CNN for Navigation Radar PPI Images," 2019 International Conference on Control, Automation and Information Sciences (ICCAIS), Chengdu, China, 2019, pp. 1-5, <https://doi.org/10.1109/ICCAIS46528.2019.9074588>.
- [9] Z. Xu, C. Fan, S. Cheng, J. Wang and X. Huang, "A Distribution Independent Ship Detector for PolSAR Images," in IEEE Journal of Selected Topics in Applied Earth Observations and Remote Sensing, <https://doi.org/10.1109/JSTARS.2021.3068843>.
- [10] J. Bai, S. Li, L. Huang and H. Chen, "Robust Detection and Tracking Method for Moving Object Based on Radar and Camera Data Fusion," in IEEE Sensors Journal, <https://doi.org/10.1109/JSEN.2021.3049449>.
- [11] V.K. Volosyuk and V.F. Kravchenko, "Statistical Theory of Radio Engineering Systems of Remote Sensing and Radar" in , Moscow:Fizmatlit, 2008.
- [12] V. K. Volosyuk and S. S. Zhyla, "Optimal radar cross section estimation in synthetic aperture radar," 2017 IEEE First Ukraine Conference on Electrical and Computer Engineering (UKRCON), Kyiv, Ukraine, 2017, pp. 189-193, <https://doi.org/10.1109/UKRCON.2017.8100471>.
- [13] V. K. Volosyuk, S. S. Zhyla, M. O. Antonov and O. A. Khaleev, "Optimal acquisition mode and signal processing algorithm in synthetic aperture radar," 2017 IEEE 37th International Conference on Electronics and Nanotechnology (ELNANO), Kiev, 2017, pp. 511-516, <https://doi.org/10.1109/ELNANO.2017.7939804>.

- [14] V. Volosyuk, S. Zhyla, N. Ruzhentsev, E. Tserne, D. Kolesnikov and D. Vlasenko, "Optimal Method of RCS Estimation in Synthetic Aperture Radar with Linear Antenna Array," 2020 IEEE Ukrainian Microwave Week (UkrMW), Kharkiv, Ukraine, 2020, pp. 1-6, <https://doi.org/10.1109/UkrMW49653.2020.9252648>.
- [15] Futatsumori, S., Morioka, K., Kohmura, A., Shioji, M. and Yonemoto, N., "Evaluation of polarisation characteristics of power-line RCS at 76 GHz for helicopter obstacle detection", *Electron. Lett.*, 51: 1110-1111 (2015).
- [16] Shunichi Futatsumori, Capucine Amielh, Kazuyuki Morioka, Akiko Kohmura, Norihiko Miyazaki, et al., "Investigation of circular polarization for 76 GHz helicopter collision avoidance radar to improve detection performance of high-voltage power lines", *EURAD 2017, 14th European Microwave Conference, Nuremberg, Germany*, pp. 295-298 (2017).
- [17] K. Sarabandi and Moonsoo Park, "A radar cross-section model for power lines at millimeter-wave frequencies," in *IEEE Transactions on Antennas and Propagation*, vol. 51, no. 9, pp. 2353-2360, Sept. 2003, <https://doi.org/10.1109/TAP.2003.816380>.
- [18] Ya. D. Shirman, "Resolution and Compression of Signals", *Sov. Radio, Moscow*, 1974.
- [19] Ya. D. Shirman, "Radioelectronic Systems: Design Foundations and Theory, 2nd ed.", *Radiotekhnika, Moscow*, 2007.
- [20] Ya. D. Shirman, "Statistical analysis of optimum resolution", *Radio Engineering and Electronics*, 6 (8), pp. 1237-1249 (1961).
- [21] V. K. Volosyuk, V. V. Pavlikov and S. S. Zhyla, "Phenomenological Description of the Electromagnetic Field and Coherent Images in Radio Engineering and Optical Systems", 2018 IEEE 17th International Conference on Mathematical Methods in Electromagnetic Theory (MMET), pp. 302-305, 2018, <https://doi.org/10.1109/MMET.2018.8460321>.
- [22] V. K. Volosyuk, S. S. Zhyla and D. V. Kolesnikov, "Phenomenological description of coherent radar images based on the concepts of the measure of set and stochastic integral", *Telecommunications and Radio Engineering (English Translation of Elektrosvyaz and Radiotekhnika)*, vol. 78, no. 1, pp. 19-30, 2019, <https://doi.org/10.1615/TelecomRadEng.v78.i1.30>.
- [23] A. Ishimaru, "SWave Propagation and Scattering in Random Media", *New York, Academic Press*, 1978.
- [24] Ya. D. Shirman, "Theoretical Foundations of Radar", *Sovetskoe radio, Moscow*, 1970.